International Journal of Mass Spectrometry 280 (2009) 26–31

Contents lists available at ScienceDirect

International Journal of Mass Spectrometry

journal homepage: www.elsevier.com/locate/ijms

Electron impact ionization of CCl_4 and SF_6 embedded in superfluid helium droplets

Harald Schöbel[a], Marcin Dampc[b], Filipe Ferreira da Silva[a], Andreas Mauracher[a], Fabio Zappa[a], Stephan Denifl[a], Tilmann D. Märk[a,1], Paul Scheier[a,*]

[a] Institut für Ionenphysik und Angewandte Physik, Universität Innsbruck Technikerstrasse 25, 6020 Innsbruck, Austria
[b] Department of Physics of Electronic Phenomena, Gdańsk University of Technology, 80-952 Gdańsk, Poland

ARTICLE INFO

Article history:
Received 6 May 2008
Received in revised form 25 June 2008
Accepted 14 July 2008
Available online 25 July 2008

We dedicate this paper to Professor Zdenek Herman on the occasion of his 75th birthday. He is has been a true friend for more than two decades and generations of students enjoyed the frequent visits of this brilliant scientist and a great teacher in our laboratories.

Keywords:
Helium droplets
CCl_4
Soft ionization

ABSTRACT

Electron impact ionization of helium nano-droplets containing several 10^4 He atoms and doped with CCl_4 or SF_6 molecules is studied with high-mass resolution. The mass spectra show significant clustering of CCl_4 molecules, less so for SF_6 under our experimental conditions. Positive ion efficiency curves as a function of electron energy indicate complete immersion of the molecules inside the helium droplets in both cases. For CCl_4 we observe the molecular parent cation CCl_4^+ that preferentially is formed via Penning ionization upon collisions with He*. In contrast, no parent cation SF_6^+ is seen for He droplets doped with SF_6. The fragmentation patterns for both molecules embedded in He are compared with gas phase studies. Ionization via electron transfer to He^+ forms highly excited ions that cannot be stabilized by the surrounding He droplet. Besides the atomic fragments F^+ and Cl^+ several molecular fragment cations are observed with He atoms attached.

1. Introduction

He droplets provide an ultra-cold temperature bath since vaporization of hot surface atoms keeps the temperature of the droplet at 0.37 K at which they are superfluid [1]. Upon collisions atoms and molecules are easily picked up by these droplets and in most cases the dopants are transferred to the center of the droplets [2]. They are quickly thermalized and form clusters inside the He droplet. The thermal energy and binding energy of the clusters transferred to the He droplet may result in the vaporization of a large number of He atoms since the binding energy of He in a droplet is 0.6 meV [3]. Helium droplets have been used for spectroscopy for many years because they offer a unique matrix for isolation of molecules [3,4].

Electron impact ionization of molecules trapped inside helium droplets has been investigated for several molecules. The projectile electrons hit with high probability a He atom on the surface or inside the droplet [5–7]. Electron transfer from neutral atoms to the ionized species transfers the charge by a random walk to the interior of the droplet where it becomes localized upon ionizing an embedded dopant molecule. The ionization energy of molecules is much lower than that of He which leads to the release of several eV of excess energy by this ionization process. In the gas phase charge transfer from He^+ to molecules often is associated with extensive fragmentation [8], however, inside a He droplet the excess energy may also be dissipated by evaporative loss of helium atoms. This can cool the parent cation and thereby reduce fragmentation [9,10].

Janda and co-workers reported for electron impact ionization of dimers of NO, that the dimer parent ion remains largely intact when ionized in helium droplets composed of >15,000 helium atoms [7]. In contrast this dimer almost exclusively decays when ionized without the surrounding He droplet. Miller and co-workers compared the fragmentation patterns upon electron impact ionization of bare triphenylmethanol with that dissolved in He droplets [11]. In addition they studied the effect of the droplet size on the reduction of fragmentation, which they called “softening”, and reported a direct but less than linear correlation of the reduction of fragmen-

* Corresponding author. Fax: +43 512 507 2932.
E-mail address: Paul.Scheier@uibk.ac.at (P. Scheier).
[1] Also at: Department Plasma Physics, Comenius University, 84248 Bratislava, Slovakia.

1387-3806/$ – see front matter © 2008 Elsevier B.V. All rights reserved.
doi:10.1016/j.ijms.2008.07.009

tation with the number of the atoms in the He droplet. Ellis and co-workers recently investigated the softening of electron impact ionization of molecules inside He droplets for haloalkanes, including CCl_4 [12] and clusters of alcohol [13,14] and ether [14]. For alcohols the most important difference to gas phase studies was a strong enhancement of the loss of a neutral H atom. Furthermore, the parent cations are more abundant for most alcohols compared with the gas phase. For the haloalkanes $CHCl_3$ and CCl_4 Ellis and co-workers could not observe a noticeable yield of the corresponding parent cations [12] which they explained by the large difference in the ionization energy of these molecules and He. Electron impact ionization of small chloroform clusters $(CHCl_3)_n$ embedded in He droplets was also investigated very recently by Denifl et al. [15]. Again no parent cations were reported but in contrast to [12] CCl_3^+ was observed with relatively high abundance. Moreover, it is interesting to note that for several atomic and a few small molecular cations He atoms attached to the ionic core have also been reported upon electron impact ionization of doped He droplets [7,16–20]. In contrast all larger molecular cations produced in this way have been observed only as bare ions.

In recent years, our group has pioneered the mass spectrometric study of electron attachment to molecules embedded in helium droplets [15,21,22]. For the chloride anion we observed a clear series of peaks where several He atoms remain attached to the anionic core [21]. In our electron attachment studies, a standard procedure in order to calibrate electron energy scales is to perform a preliminary experiment with either CCl_4 or SF_6 [23,24]. The importance of SF_6 and CCl_4 as calibrants for basically all electron attachment studies motivates the investigation of these molecules embedded in He droplets [25]. For all electron attachment studies in doped He droplets [15,21,22] we probe the cluster size distributions first in the positive ion mode. Electron impact ionization studies to He droplets doped with both molecules were published previously by other authors [9,12]. The present results will be compared with these earlier investigations [9,12] and special emphasis is given to the stabilization of parent cations and product ions that have He atoms attached. In order to separate ions with nominally the same mass per charge ratio but with different composition the 2-sector field mass spectrometer is operated in high-mass resolution mode.

2. Experimental setup

Since the main parts of the experimental set-up have already been described elsewhere [26,27], we will give here just a short overview. The helium droplets are formed by supersonic expansion of high-pressure (23 bar), high-purity helium gas (>99.9999%), which passes through a 5 μm aperture into vacuum. Before expansion, the gas is additionally cleaned and pre-cooled by a liquid-nitrogen cold trap and cooled down to ∼10 K by a closed cycle helium cryostat. The pressure in the chamber where expansion takes place is kept below 10^{-2} Pa by a 1200 l/s turbo-molecular pump. Under these conditions, the average droplet size is expected to be several 10^4 atoms [3].

The flow of the helium droplets and He gas emerging from the aperture is skimmed 10 mm downstream to block most of the He gas while letting through the inner, colder part of the expansion plume. The unperturbed central beam of helium droplets then passes into another vacuum chamber that contains a small pick-up cell. This cell is approximately 10 cm long and 5 cm wide, and has at the entrance and exit 5 mm apertures to allow the passage of the helium droplet beam. The pressure of gas inside the pick-up cell is estimated indirectly by the pressure of the vacuum chamber that contains it, which in turn is pumped by a 260 l/s turbo-molecular pump, reaching a base pressure of 10^{-5} Pa when the cell is not operated and the He beam is on. The sample of CCl_4 (Sigma–Aldrich, stated purity 99.95%) liquid is placed in a small stainless steel tube that is connected to the gas line of the pick-up cell with a needle valve. Several freeze-pump cycles are performed to remove atmospheric contamination from the container. CCl_4 has a sufficiently high-vapor pressure that it is sufficient to open the needle valve with the liquid at room temperature to produce an adequate flow of molecules into the collision cell. SF_6 (Linde, stated purity of 99.999%) is already a gas and the introduction to the pick-up cell is straightforward. Optimum conditions (yield) are obtained for a dopant pressure between 10^{-3} and 2×10^{-3} Pa in the pick-up cell.

After the passage through a second skimmer, the helium droplets enter another vacuum chamber where they intersect an electron beam of a Nier-type ion source. The energy resolution of the electron gun is around 1 eV, while the electron current is set to 400 μA for measuring mass spectra and 20 μA for measuring ion efficiency curves. The mass spectrometer is a modified 2-sector field Varian-MAT CH5, which provides a mass resolution $\Delta m/m$ of around 200 with open slits (ion efficiency curves) and about 1000 with closed slits (mass spectra).

3. Results and discussion

3.1. CCl_4

In Fig. 1 we present a high-resolution mass spectrum of the positive ions formed upon electron impact ionization of He droplets doped with CCl_4. The upper diagram shows the mass range from 28 to 180 Thomson which includes signals of the low-mass fragment Cl^+ up to the monomer ion CCl_4^+. The most prominent peaks are the fragments CCl_3^+ and CCl_2^+. The middle diagram shows the mass range from 180 to 330 Thomson. Also for the dimeric cations the most abundant ions are the fragments formed upon loss of one and two chlorine atoms. The mass spectrum was measured at an electron energy of 120 eV and an electron current of 400 μA. The He droplet source was operated at a pressure of 23 bar and a nozzle temperature of 10 K. The mass resolution was set to a value of $m/\Delta m \sim 1000$ which is sufficiently high to separate product ions of CCl_4 from He_n^+ and hydrocarbon ions, originating from the residual gas, due to the large different deviations from unit mass between H (1.0078 Da) and He (4.0026 Da) compared to ^{12}C (12 Da) and ^{35}Cl (34.9689 Da) [28]. Up to the fragment ion CCl_2^+ the mass spectrum is dominated by pristine He_n^+ cluster ions (masses of multiple of 4). Note that in Fig. 1 the CCl_4^+ parent ion cannot be seen immediately (see below). This is consistent with electron impact ionization of bare CCl_4 [29]. For CCl_4 and CF_4 Deutsch et al. [30] reported a weak metastable decay of the parent cations loosing a halogen atom a few microseconds after the ionization process. Shortly thereafter, a very weak signal for CCl_4^+ was observed in the mass spectrum of CCl_4 by other authors [31–33]. Drewello et al. [32] reported the kinetic energy release for metastable Cl-loss to be large (160 meV). In [33] the relative abundance of the parent cation is reported to be $3.5 \pm 0.5 \times 10^{-6}$ of the most abundant fragment CCl_3^+ (117 Da, base peak).

Figs. 2–4 show enlarged sections of the CCl_4 mass spectrum of Fig. 1. All product ions of CCl_4 are compared with the corresponding calculated isotopic pattern shown as open bars. The upper diagram of Fig. 2 shows the two isotopes of Cl^+ (open bars with solid line) and HCl^+ (open bars with dashed line). The latter ion is a product upon ionization of doped He droplets that contain traces of water. The relatively large abundance of HCl^+ indicates a high efficiency for the formation of this reaction product inside the He droplets. Furthermore, water or its fragments attached to other product ions of CCl_4 are present only as extremely weak signals in the mass spec-

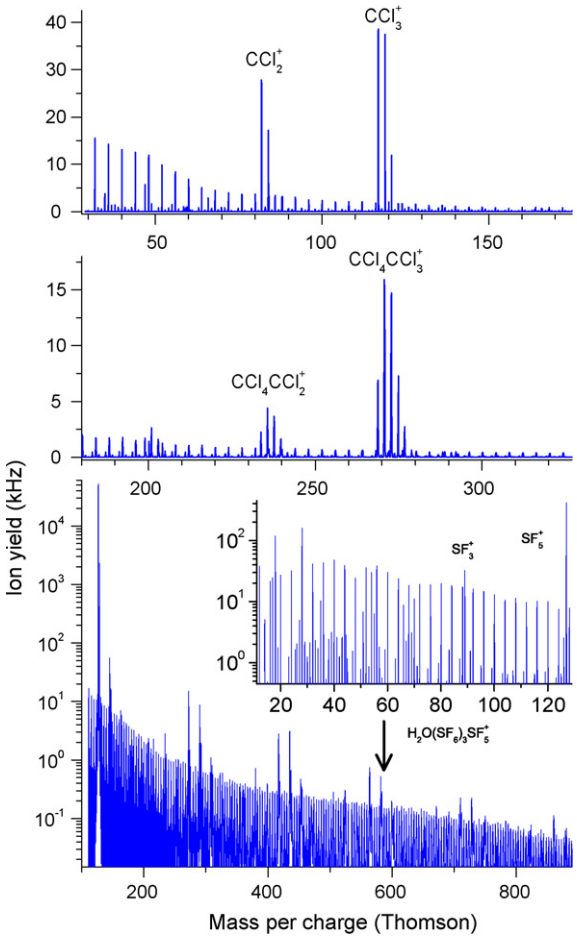

Fig. 1. Upper and middle diagram: positive ion mass spectra of He droplets doped with CCl_4. Electron energy 120 eV, electron current 400 μA, CCl_4 pressure 2×10^{-3} Pa, 23 bar He and 10 K. Lower diagram: positive ion mass spectrum of He droplets doped with SF_6. Clusters of the form $(SF_6)_nSF_3^+$, $(SF_6)_nSF_5^+$ and $(H_2O)_m(SF_6)_nSF_5^+$ are peaking out of the He_n^+ series. Electron energy 120 eV, electron current 400 μA, 23 bar He and 10 K. For the long mass range spectrum the SF_6 pressure was set to 2×10^{-3} Pa and all slits were kept open. For the inset the SF_6 pressure was set to 5×10^{-4} Pa and the mass resolution was increased by closing the slits to a value of $m/\Delta m \sim 1000$.

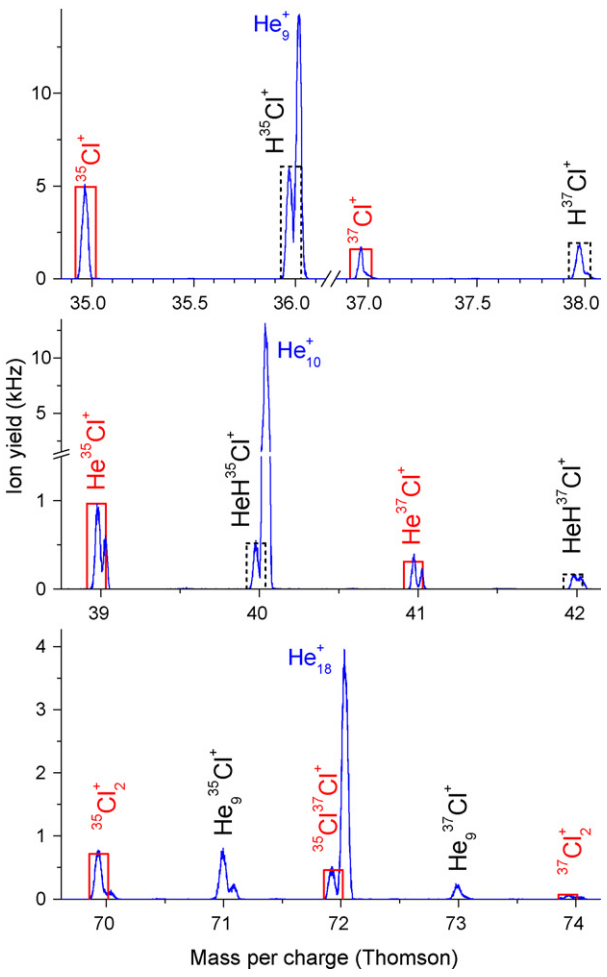

Fig. 2. Enlarged sections of the positive ion mass spectrum of He droplets doped with CCl_4 shown in Fig. 1. The upper diagram shows the ions Cl^+ and HCl^+. The latter ion is formed upon ionization of droplets containing CCl_4 and traces of H_2O. The center diagram shows $HeCl^+$ and $HeHCl^+$ and the lower diagram Cl_2^+. Electron energy 120 eV, electron current 400 μA, CCl_4 pressure 2×10^{-3} Pa, 23 bar He and 10 K.

trum. It is remarkable that besides Cl^+ also HCl^+ quite efficiently binds He atoms (see center diagram). Moreover, Cl_2^+ (see lower diagram of Fig. 2) is formed from doped He droplets with almost 2% of the most intense product, i.e., CCl_3^+ and its existence is not reported in the gas phase mass spectrum taken from the literature [29]. Cl_3^+ is formed in the doped He droplets as well with about an order of magnitude less intensity. The formation of the Cl_3^+ cation was reported in the literature by chlorine chemical ionization via the exothermic reaction of Cl^+ transfer from Cl_2^{2+} to chlorine or by the endothermic reaction of Cl_2^+ with chlorine [34]. In He droplets doped with clusters of CCl_4 the same reactions are likely to occur as Cl_2 and Cl_2^+ can be formed via collisions of CCl_4 with He^+ and He^*.

Fig. 3 shows the non-fragmented monomer (upper diagram) and dimer (lower diagram) cations of CCl_4. The close distance of $C^{35}Cl_4^+$ and $C^{35}Cl_2{}^{37}Cl_2^+$ to the relatively intense He clusters He_{38}^+ and He_{39}^+, respectively, results due to the limited resolution only in shoulders at the low-mass side of the He cluster peaks for these parent cations. However, the yield of these shoulders as well as the other more accessible peaks match perfectly well with the calculated isotopic pattern of CCl_4. The total yield of the monomer cation is about 0.3% of the yield of CCl_3^+ which is about three orders of magnitude higher than the value reported earlier for the gas phase [33]. For the dimer cation more peaks can be identified and the yield of this product cation relative to the most intense dimer ion, i.e., $CCl_4CCl_3^+$ is 0.2%. Fig. 4 shows in addition two examples of dimeric fragment ions that can only be identified with high-mass resolution.

In the upper diagram of Fig. 5 the relative abundance of all monomeric (solid bars) and dimeric (open bars) product cations are plotted and compared to the data calculated from the gas phase mass spectrum taken from [29] (hatched bars). In order to account for the different isotopic patterns the ratios were derived from the sum of all isotopomers divided by the sum of all corresponding product ion peaks. It is interesting to note that the present values for CCl^+, CCl_2^+ and CCl_3^+ (monomeric fragments) agree extremely well (better than 10%) with the values published by Ellis and co-workers for He droplets doped with CCl_4. In He droplets the fragment CCl_2^+ is formed about five times more abundantly compared to the gas phase. Furthermore, the ions Cl_2^+, Cl_3^+ and CCl_4^+ are not formed (or extremely weak) in gas phase experiments. In addition, also Cl^+ is more efficiently formed in He droplets. Thus, electron impact of He droplets doped with CCl_4 forms carbon-free chlorine with higher abundance compared to gas phase which means that more

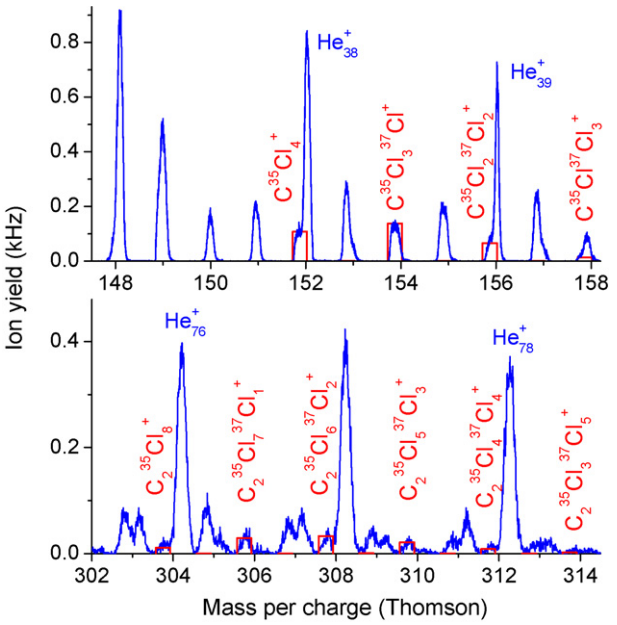

Fig. 3. Enlarged sections of the positive ion mass spectrum of He droplets doped with CCl_4 shown in Fig. 1. The upper diagram shows the parent ion CCl_4^+ and the lower diagram the dimer $(CCl_4)_2^+$. Electron energy 120 eV, electron current 400 μA, CCl_4 pressure 2×10^{-3} Pa, 23 bar He and 10 K.

C–Cl bonds are broken in the droplet. Parallel carbon rich fragments such as CCl^+ and CCl_2^+ show reduced yield when formed in doped droplets compared to the gas phase.

Furthermore, Fig. 6 shows the threshold region of the ion efficiency curves of CCl_4^+ (solid squares) and $CCl_4CCl_2^+$ (solid circles) measured with an electron current of 20 μA. The electron energy scale is calibrated with the threshold of the ion efficiency curve of He measured under the same conditions. Both ions show the presence of two common formation processes, a weak contribution with a threshold close to 20 eV and a dominant channel with a threshold around 25 eV. The latter can be assigned to the reaction sequence where a He atom (ionization energy 24.58 eV [29]) is ionized and the charges move by random hopping to the center

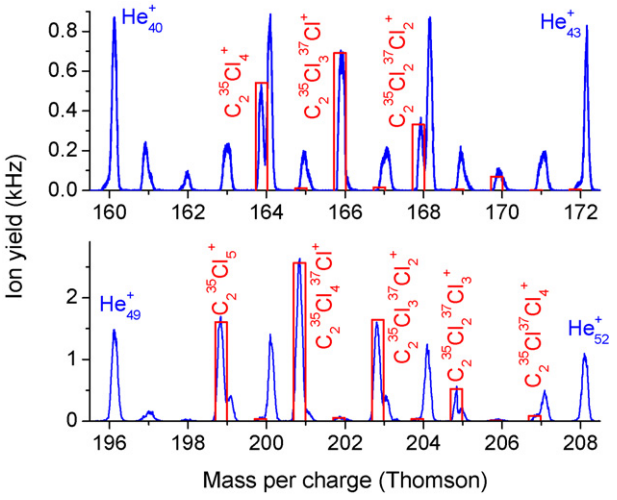

Fig. 4. Enlarged sections of the positive ion mass spectrum of He droplets doped with CCl_4 shown in Fig. 1. The upper diagram shows the section around the cluster fragment $C_2Cl_4^+$. The lower diagram shows the section around the cluster fragment $C_2Cl_5^+$. Electron energy 120 eV, electron current 400 μA, CCl_4 pressure 2×10^{-3} Pa, 23 bar He and 10 K.

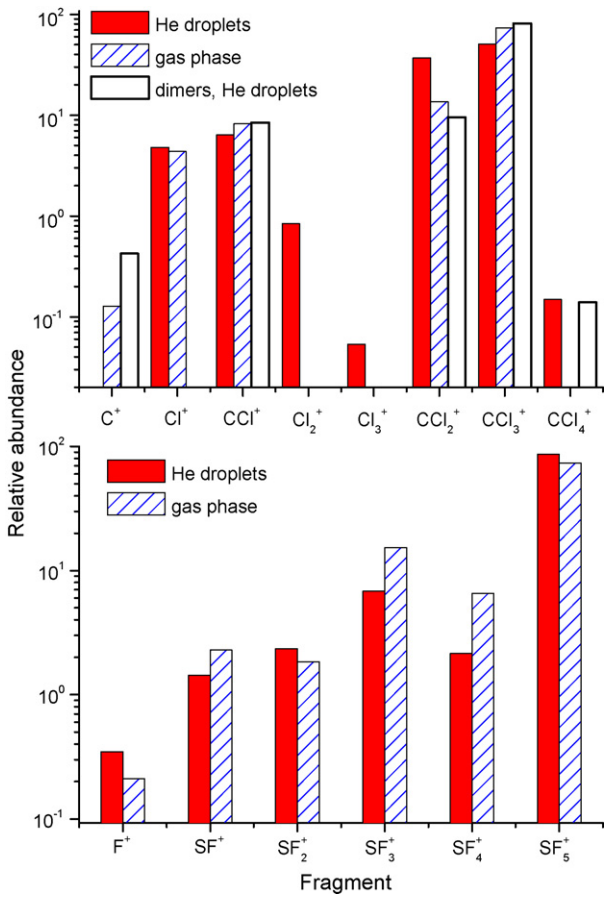

Fig. 5. Product ions formed upon electron impact ionization of CCl_4 (upper diagram) and SF_6 (lower diagram). The values are normalized to the sum of the corresponding product ion yields. The values in the graph represent the sum of all isotopomers. The solid bars represent the monomeric and the open bars the dimeric products from doped He droplets. The dashed bars are derived from the gas phase mass spectrum published in [29].

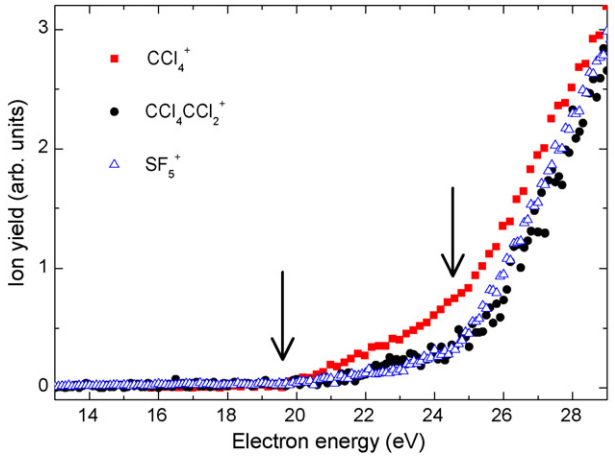

Fig. 6. Ion efficiency curves as a function of the incident electron energy for fragment ions formed upon electron impact of He droplets doped with CCl_4 (solid symbols) and SF_6 (open triangles). For all ions two thresholds at slightly below 20 eV and at about 25 eV can be identified and are indicated as vertical arrows. In comparison the ion efficiency curve of He_{38}^+ is an isobaric ion to CCl_4^+ ($m/z \sim 152$ Thomson). Both ions were separated completely with closed slits.

where a highly exothermic charge transfer reaction to CCl_4 takes place [5–7]. At electron energies above 70 eV this process is by far the dominating channel. The appearance energy of the most abundant fragment ion CCl_3^+ is 11.47 eV [29] and thus an excess energy of 14 eV has to be shared in this ionization process among the two initially formed fragments, i.e., $Cl^\bullet$ and CCl_3^+. A substantial part of this energy will remain in the polyatomic fragment and may break further C–Cl bonds. The high amount of Cl_n^+ ($n = 1, 2$ and 3) and the reduced yield of CCl_3^+ products from doped He droplets (see Fig. 5 upper diagram) support this explanation and indicate that cooling by the He droplet is not fast enough to stabilize the highly excited CCl_3^+ intermediate.

The production of CCl_4^+ with a threshold of about 20 eV, we assign as Penning ionization of CCl_4 via electronically excited He*. This process is operative for electron energies higher than about 20 eV. In contrast to the electron transfer reaction to He^+ described above the energy difference between He* and CCl_4 can be carried away by the emitted electron which leads to the formation of substantially less excited ions, similar to electron impact ionization of bare CCl_4 where lifetimes of CCl_4^+ in the order of μs were reported [30–33]. Delayed fragmentation reactions are strongly suppressed by the efficient cooling of the surrounding He droplet which in the present case stabilizes CCl_4^+ being formed upon Penning ionization via He*. CCl_4^+ is also formed via the electron transfer to He^+, however, compared to all other product ions this channel is less important.

The upper diagram of Fig. 7 shows ions of the form He_nX^+ (with $n = 0$–20) where X is a product ion of CCl_4. For Cl^+ both isotopes

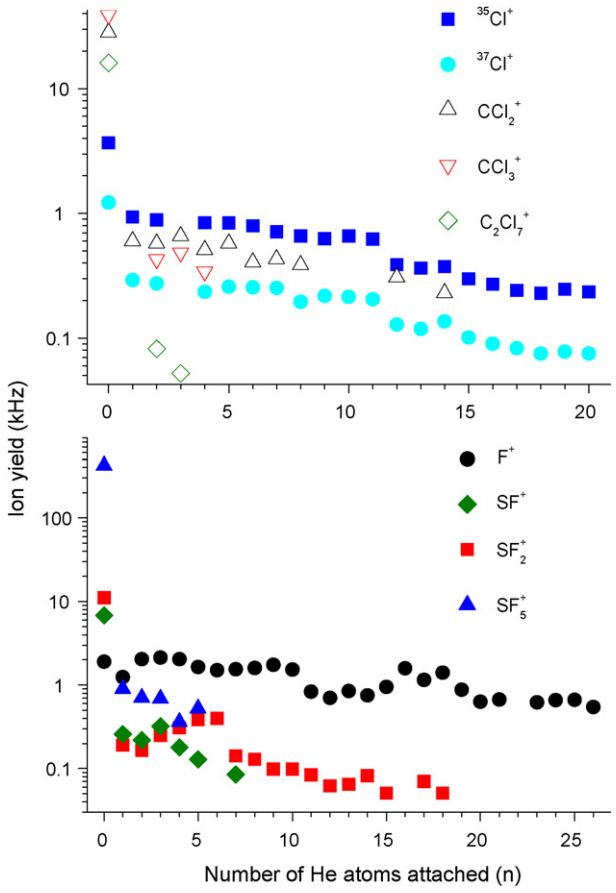

Fig. 7. Ion yield of the product ions of He droplets doped with CCl_4 (upper diagram) and SF_6 (lower diagram) that bind He atoms as a function of the number of the He atoms attached.

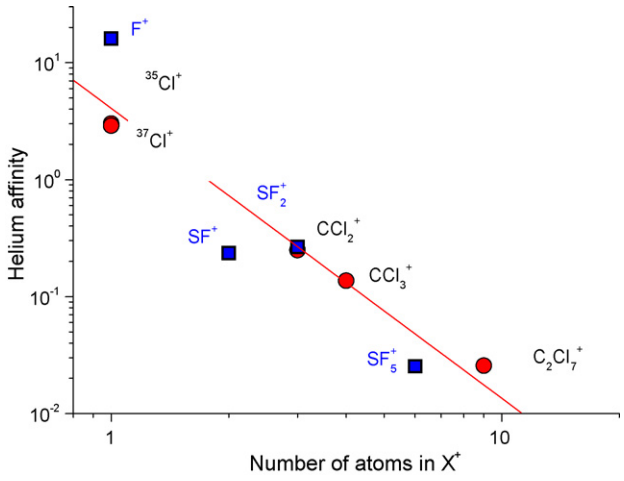

Fig. 8. Helium affinity calculated via Eq. (1) for all product ions X^+ formed upon electron impact ionization of He droplets doped with CCl_4 (circles) and SF_6 (squares) plotted as a function of the number of atoms in the bare cation X^+.

dissolve in He equally well which is reflected in the constant shift between the two corresponding curves in the semi-logarithmic plot. From $n = 11$–12 the intensity of the chlorine cations dissolved in He drops by almost an order of magnitude, thus indicating the closure of a first shell at $n = 11$. This is different from a coordination number of 12 that can be assigned to an icosahedral structure which often is observed for pristine rare gas cluster ions [35–37].

We define the helium affinity (HA) of a given ion X^+ as the ratio of the sum of the ion yields of all ions He_nX^+ ($n \geq 1$) and the yield of the bare ion X^+:

$$\mathrm{HA}(X^+) = \frac{\sum_{n\geq 1} i(\mathrm{He}_n X^+)}{i(X^+)} \quad (1)$$

Fig. 8 shows the helium affinity of product ions X^+ of He droplets doped with CCl_4 and SF_6. All X^+ ions binding at least one He atom that can be identified in the high-resolution mass spectra for CCl_4 (Fig. 1, upper diagram) and SF_6 (Fig. 1 inset of the lower diagram) doped He droplets are included in Fig. 8. The helium affinity nonlinearly depends on the number of atoms of the X^+ ion and is largest for atomic ions in agreement with the literature [7,16–20]. It is interesting to note that the relative abundance of bare ions with a high-helium affinity is increased in He droplets compared to that for electron impact ionization of gas phase molecules.

3.2. SF_6

The lower diagram of Fig. 1 shows a mass spectrum of cations formed upon electron impact ionization of He droplets doped with SF_6. The electron energy was set to 120 eV, the electron current was 400 μA and all slits were fully open which results in a mass resolution $m/\Delta m \sim 200$. The conditions of the He cluster source were 23 bar He pressure and 10 K nozzle temperature. The pressure of SF_6 in the pick-up chamber was 2×10^{-3} Pa. The most abundant product by far is SF_5^+. 18 mass units higher the ion $H_2O{\cdot}SF_5^+$ can be identified. Another 18 mass units higher even two water molecules attached to SF_5^+ can be identified. The yield of these hydrated species is surprisingly high and we checked three different cylinders of SF_6 and two different gas inlets to identify the source of this water contamination. Apparently it is originating from the residual gas, however, for other systems like CCl_4 (see above) the relative abundance of hydrated ions is much lower. Clusters of the form $(SF_6)_nSF_5^+$ and their hydrated species are also visible in Fig. 1

(lower diagram) up to $n = 5$. For clusters hydration becomes much more abundant. The inset in the lower diagram of Fig. 1 shows the low-mass range up to SF_5^+ measured with high-mass resolution. In addition the SF_6 pressure in the pick-up chamber was reduced to 5×10^{-4} Pa. This minimizes the flow of bare SF_6 molecules into the ion source.

The lower diagram of Fig. 5 shows the relative abundance of the product ions formed upon electron impact ionization of bare SF_6 and that from He droplets doped with SF_6 (taken from the inset of the lower diagram of Fig. 1). For each fragment ion the ion yield (sum of all isotopomers) was normalized with the sum of the ion yield of all fragment ions of SF_6 up to the mass of SF_5^+. The solid bars represent the fragment ions of SF_6 from doped He droplets. The dashed bars are derived from the gas phase mass spectrum published in [29]. In contrast to CCl_4 (see above) and some earlier studies on SF_6 in the literature [9] we do not observe the parent cation SF_6^+ within the limits of the sensitivity of our experiment ($<10^{-8}$ of the most intense fragment SF_5^+). This agrees well with photoionization experiments of He droplets doped with SF_6 [38]. SF_4^+ and SF_3^+ are strongly reduced when formed from doped He droplets compared to electron impact ionization of gas phase molecules. At the same time F^+, SF_2^+ and SF_5^+ are slightly enhanced.

The mass spectrum shown in the inset of the lower diagram of Fig. 1 is measured with sufficiently high-mass resolution to distinguish isobaric fragments of the form He_nX^+ with $X = F^+$, SF^+, SF_2^+ and SF_5^+ from other ions in the mass spectrum including pristine He cluster cations and ions originating from the residual gas. As in the case of CCl_4 all ions that are formed with higher abundance in doped He droplets compared to electron impact ionization of gas phase SF_6 bind He atoms. Although SF_3^+ and SF_4^+ are formed more efficiently than F^+ it is impossible to observe $He_nSF_3^+$ or $He_nSF_4^+$ within the detection limit of the instrument. In Fig. 8 the helium affinities for SF_3^+ and SF_4^+ are at least two orders of magnitude lower than that of SF_5^+. The lower diagram of Fig. 7 shows the ion yield of product ions of SF_6 that bind He as a function of the number of He atoms attached. Like in the case of CCl_4 the atomic halogen ion F^+ has the highest affinity to bind He atoms. The ion yield of He_nF^+ drops clearly for $n > 10$, thus indicating a shell closure at $n = 10$ which again does not match with an icosahedral shell closure. The He affinity of F^+ is almost an order of magnitude higher than that of Cl^+ (see Fig. 8). However, molecular product ions of SF_6 have a lower He affinity compared to molecular CCl_4 product ions. The line in the double logarithmic plot in Fig. 8 is a linear fit to the helium affinities of all product ions of SF_6 and CCl_4 that bind at least one He atom.

4. Conclusions

We have presented an exploratory study on positive ion formation by electron impact on helium droplets doped with CCl_4 and SF_6. For CCl_4 the parent cation CCl_4^+ can be stabilized efficiently by the surrounding He, especially if the ion is formed via Penning ionization. However, charge transfer from He^+ breaks more C–Cl bonds compared to electron impact ionization of bare CCl_4 molecules. SF_6^+, however, cannot be stabilized if ionized in He droplets independent on the ionization mechanism operative, i.e., Penning ionization and electron transfer to He^+. Besides the atomic fragments F^+ and Cl^+ several molecular fragment cations are observed with He atoms attached. Ions with a high affinity to He are enhanced as bare ions formed from doped He droplets compared to electron impact ionization of gas phase molecules. In addition the present work provides important information required for an upcoming study about negative ion formation of He droplets doped with CCl_4 and SF_6, two of the most intensely investigated molecules concerning electron attachment. Besides knowledge about the size distribution of clusters of dopant molecules inside the He droplets inelastic scattering and Penning ionization are two reaction channels that provide secondary electrons in the energy range where attachment reactions are operative [39].

Acknowledgments

This work has been supported by the FWF, Wien, Austria, and the European Commission, Brussels. F.Z. gratefully acknowledges a Post-doc Grant from the Brazilian agency CNPq, S.D. an APART Grant from the Austrian Academy of Sciences and M.D. a visiting fellowship from EIPAM.

References

[1] S. Grebenev, J.P. Toennies, A.F. Vilesov, Science 279 (1998) 2083.
[2] M.Y. Choi, G.E. Douberly, T.M. Falconer, W.K. Lewis, C.M. Lindsay, J.M. Merritt, P.L. Stiles, R.E. Miller, Int. Rev. Phys. Chem. 25 (2006) 15.
[3] J.P. Toennies, A.F. Vilesov, Angew. Chem. Int. Ed. 43 (2004) 2622, and references cited therein.
[4] J. Tiggesbäumker, F. Stienkemeier, Phys. Chem. Chem. Phys. 9 (2007) 4748.
[5] H. Buchenau, J.P. Toennies, J.A. Northby, J. Chem. Phys. 95 (1991) 8134.
[6] J. Seong, K.C. Janda, N. Halberstadt, F. Spiegelmann, J. Chem. Phys. 109 (1998) 10873.
[7] B.E. Callicoatt, D.D. Mar, V.A. Apkarian, K.C. Janda, J. Chem. Phys. 105 (1996) 7872.
[8] T.L. Williams, L.M. Babcock, N.G. Adams, Int. J. Mass Spectrom. 185–187 (1999) 759.
[9] A. Scheidemann, B. Schilling, J.P. Toennies, J. Phys. Chem. 97 (1993) 2128.
[10] A. Boatwright, J. Jeffs, A.J. Stace, J. Phys. Chem. A 111 (2007) 7481.
[11] W.K. Lewis, B.E. Applegate, J. Sztáray, B. Sztáray, T. Baer, R.J. Bemish, R.E. Miller, J. Am. Chem. Soc. 126 (2004) 11283.
[12] S. Yang, S.M. Brereton, M.D. Wheeler, A.M. Ellis, J. Phys. Chem. A 110 (2006) 1791.
[13] S. Yang, S.M. Brereton, A.M. Ellis, Int. J. Mass Spectrom. 253 (2006) 79.
[14] S. Yang, S.M. Brereton, M.D. Wheeler, A.M. Ellis, Phys. Chem. Chem. Phys. 7 (2005) 4082.
[15] S. Denifl, F. Zappa, I. Mähr, A. Mauracher, M. Probst, T.D. Märk, P. Scheier, J. Am. Chem. Soc. 130 (2008) 5065.
[16] A.A. Scheidemann, V.V. Kresin, H. Hess, J. Chem. Phys. 107 (1997) 2839.
[17] B.E. Callicoatt, K. Förde, T. Ruchti, L. Jung, K.C. Janda, N. Halberstadt, J. Chem. Phys. 108 (1998) 9371.
[18] T. Ruchti, K. Förde, B.E. Callicoatt, H. Ludwigs, K.C. Janda, J. Chem. Phys. 109 (1998) 10679.
[19] T. Ruchti, B.E. Callicoatt, K.C. Janda, Phys. Chem. Chem. Phys. 2 (2000) 4075.
[20] M. Farnik, J.P. Toennies, J. Chem. Phys. 122 (2005) 014307.
[21] S. Denifl, F. Zappa, I. Mähr, J. Lecointre, M. Probst, T.D. Märk, P. Scheier, Phys. Rev. Lett. 97 (2006) 043201.
[22] F. Zappa, S. Denifl, I. Mähr, A. Bacher, O. Echt, T.D. Märk, P. Scheier, J. Am. Chem. Soc. 130 (2008) 5573.
[23] D. Huber, M. Beikircher, S. Denifl, F. Zappa, S. Matejcik, A. Bacher, V. Grill, T.D. Märk, P. Scheier, J. Chem. Phys. 125 (2006) 084304.
[24] S. Ptasinska, S. Denifl, S. Gohlke, P. Scheier, E. Illenberger, T.D. Märk, Angew. Chem. Int. Ed. 45 (2006) 1893.
[25] Electron attachment studies to He droplets doped with SF_6 and CCl_4 will be the subject of an upcoming study.
[26] S. Denifl, M. Stano, A. Stamatovic, P. Scheier, T.D. Märk, J. Chem. Phys. 124 (2006) 054320.
[27] S. Feil, K. Gluch, S. Denifl, F. Zappa, O. Echt, P. Scheier, T.D. Märk, Int. J. Mass. Spectrom. 252 (2006) 166.
[28] G. Audi, A.H. Wapstra, C. Thibault, Nucl. Phys. A 729 (2003) 337.
[29] NIST Chemistry WebBook. http://webbook.nist.gov/chemistry/.
[30] H. Deutsch, K. Leiter, T.D. Märk, Int. J. Mass Spectrom. Ion Proc. 67 (1985) 191.
[31] L.A. Shadoff, Org. Mass Spectrom. 21 (1986) 381.
[32] T. Drewello, T. Weiske, H. Schwarz, Angew. Chem. Int. Ed. Engl. 24 (1985) 869.
[33] C.E.C.A. Hop, J.L. Holmes, F.P. Lossing, J.K. Terlouw, Int. J. Mass Spectrom. Ion Proc. 83 (1988) 285.
[34] F. Cacace, G. de Petris, F. Pepi, M. Rosi, A. Sgamellotti, Rapid Commun. Mass Spectrom. 12 (1998) 1911.
[35] O. Echt, K. Sattler, E. Recknagel, Phys. Rev. Lett. 47 (1981) 1121.
[36] P. Scheier, T.D. Märk, Int. J. Mass Spectrom. Ion Proc. 102 (1990) 19.
[37] T.D. Märk, P. Scheier, J. Chem. Phys. 87 (1987) 1456.
[38] R. Fröchtenicht, U. Henne, J.P. Toennies, A. Ding, M. Fieber-Erdmann, T. Drewello, J. Chem. Phys. 104 (1996) 2548.
[39] H. Schöbel et al., submitted for publication.